Analysis of GTP addition in the reverse (3′–5′) direction by human tRNA^{His} guanylyltransferase

AKIYOSHI NAKAMURA,[1] DAOLE WANG,[2] and YASUO KOMATSU[2,3]

[1]Bioproduction Research Institute, National Institute of Advanced Industrial Science and Technology (AIST), Tsukuba, Ibaraki 305-8565, Japan
[2]Graduate School of Life Science, Hokkaido University, Sapporo 060-0810, Japan
[3]Cellular and Molecular Biotechnology Research Institute, National Institute of Advanced Industrial Science and Technology (AIST), Tsukuba, Ibaraki 305-8565, Japan

ABSTRACT

Human tRNA^{His} guanylyltransferase (HsThg1) catalyzes the 3′–5′ addition of guanosine triphosphate (GTP) to the 5′-end (−1 position) of tRNA^{His}, producing mature tRNA^{His}. In human cells, cytoplasmic and mitochondrial tRNA^{His} have adenine (A) or cytidine (C), respectively, opposite to G_{-1}. Little attention has been paid to the structural requirements of incoming GTP in 3′–5′ nucleotidyl addition by HsThg1. In this study, we evaluated the incorporation efficiencies of various GTP analogs by HsThg1 and compared the reaction mechanism with that of *Candida albicans* Thg1 (CaThg1). HsThg1 incorporated GTP opposite A or C in the template most efficiently. In contrast to CaThg1, HsThg1 could incorporate UTP opposite A, and guanosine diphosphate (GDP) opposite C. These results suggest that HsThg1 could transfer not only GTP, but also other NTPs, by forming Watson–Crick (WC) hydrogen bonds between the incoming NTP and the template base. On the basis of the molecular mechanism, HsThg1 succeeded in labeling the 5′-end of tRNA^{His} with biotinylated GTP. Structural analysis of HsThg1 was also performed in the presence of the mitochondrial tRNA^{His}. Structural comparison of HsThg1 with other Thg1 family enzymes suggested that the structural diversity of the carboxy-terminal domain of the Thg1 enzymes might be involved in the formation of WC base-pairing between the incoming GTP and template base. These findings provide new insights into an unidentified biological function of HsThg1 and also into the applicability of HsThg1 to the 5′-terminal modification of RNAs.

Keywords: transfer RNA (tRNA); aminoacyl tRNA synthetase; RNA modification; 3′-5′ polymerase; RNA structure

INTRODUCTION

The enzymes tRNA^{His} guanyltransferase (Thg1) and Thg1-like protein (TLP) catalyze the addition of nucleotides to the 5′-end of tRNA in the reverse direction (3′–5′) (Heinemann et al. 2012; Jackman et al. 2012; Chen et al. 2019). In the cytoplasm of eukaryotes Thg1 catalyzes the addition of a guanosine residue to the 5′-end of tRNA^{His} (Gu et al. 2003) at the −1 position (G_{-1}), which serves as a major recognition element of histidyl-tRNA synthetase (HisRS) (Cooley et al. 1982; Himeno et al. 1989; Rudinger et al. 1994; Rosen and Musier-Forsyth 2004), with rare exceptions (Rao and Jackman 2015; Lee et al. 2019). Thg1 recognizes a His anticodon (GUG) in a 5′-monophosphorylated tRNA^{His} (p-tRNA^{His}), which is cleaved by RNase P from pre-tRNA^{His} (Jackman and Phizicky 2006). The Thg1-catalyzed G_{-1} addition reaction involves three steps (Jahn and Pande 1991; Gu et al. 2003). In the first step, the p-tRNA^{His} is activated by ATP to produce a 5′-adenylylated-tRNA^{His} intermediate. In the second step, the 3′-OH of an incoming GTP attacks the 5′–5′ phosphate linkage of the intermediate, to produce a 5′-triphosphorylated G_{-1}-tRNA^{His} intermediate (pppG_{-1}-tRNA^{His}). In the third step, the pyrophosphate group is removed from the intermediate pppG_{-1}-tRNA^{His} to generate mature 5′-monophosphorylated G_{-1}-tRNA^{His} (pG_{-1}-tRNA^{His}). TLPs have been identified in several organisms, including archaea, bacteria, and mitochondria (Abad et al. 2010; Heinemann et al. 2010), and have been shown to catalyze the addition of 5′-terminal nucleotides to truncated tRNAs by a similar reaction process as that of Thg1, with a broader range of substrate specificity (Abad et al. 2011; Rao et al. 2011; Long et al. 2016; Dodbele et al. 2019).

Abbreviations: tRNA, transfer RNA; Thg1, tRNA^{His} guanyltransferase; TLP, Thg1-like protein; HisRS, histidyl-tRNA synthetase; WC, Watson–Crick

Corresponding author: komatsu-yasuo@aist.go.jp

Article is online at http://www.rnajournal.org/cgi/doi/10.1261/rna.078287.120.

G_{-1} is also found in the $tRNA^{His}$ of mammalian mitochondria, possibly added post-transcriptionally (Suzuki and Suzuki 2014). Human mitochondrial HisRS requires the G_{-1} of mitochondrial $tRNA^{His}$ for efficient aminoacylation (Lee et al. 2017). Recently, it has been demonstrated that human Thg1 (HsThg1) catalyzes G_{-1} addition reactions in both human cytoplasmic (hc) and mitochondrial (hm) $tRNA^{His}$. This observation suggests that HsThg1 could participate in both cytoplasmic and mitochondrial $tRNA^{His}$ maturation (Nakamura et al. 2018a). In the cytoplasm of eukaryotes, Thg1 adds G_{-1} to the 5′-end of $hctRNA^{His}$, opposite a conserved A_{73}, resulting in a G:A 3′–5′ mismatch addition reaction. $hmtRNA^{His}$ contains a cytosine residue opposite the G_{-1}. Although a single G_{-1} has been observed at the 5′-end of $hmtRNA^{His}$ in mitochondria, multiple guanosines were incorporated into the 5′-end of $hmtRNA^{His}$ by HsThg1 in vitro, suggesting that a currently unidentified mechanism is required to prevent the addition of multiple GTPs in vivo.

The structure–function relationship of incoming GTP with four types of opposite residues—A, C, G, and U—in *Candida albicans* Thg1 (CaThg1) was analyzed using several GTP analogs and a newly developed two-piece $tRNA^{His}$ composed of a 5′-short primer (5′RF) and the remaining 3′ template RNA strands (3′RF) (Nakamura et al. 2018b). A non-Watson–Crick (WC) G:A base pair can be formed between incoming GTP and A_{73}, and may contribute to the prevention of continuous templated 3′–5′ polymerization, resulting in accurate single G_{-1} addition. However, the nucleotide recognition mechanism of HsThg1, which participates in the maturation of both $hctRNA^{His}$ and $hmtRNA^{His}$, depending on whether the opposite residue is A or C, is still unclear.

In this study, we evaluated the efficiency of incorporation by HsThg1 of various nucleotide analogs into the −1 position. The results suggested the existence of a broad range of mechanisms for substrate recognition by HsThg1. We used HsThg1 for 5′-end labeling of single-stranded RNA with modified GTP analogs, such as biotinylated GTP. We also performed the structural analysis of HsThg1 in the presence of $hmtRNA^{His}$ and found that the structural diversity of the carboxy-terminal domain of the Thg1 enzymes may be associated with WC base-pairing in 3′–5′ nucleotide addition.

RESULTS AND DISCUSSION

HsThg1 can transfer GTP to the 5′-end of two-piece $tRNA^{His}$

We previously divided $tRNA^{His}$ into a 13 mer 5′-side RNA fragment (5′RF) and a 64 mer 3′-side RNA fragment (3′RF)

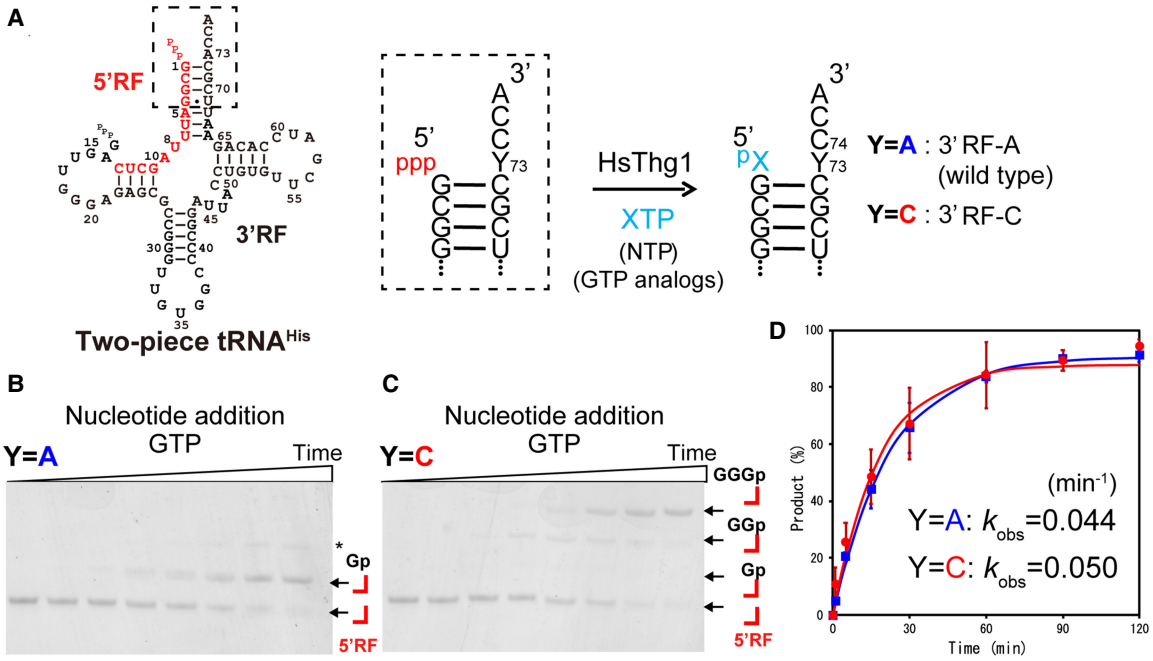

FIGURE 1. Nucleotide addition reaction by HsThg1 onto a two-piece $tRNA^{His}$. (*A*) Reaction scheme of a nucleotide addition reaction with natural NTPs and various GTP analogs (XTP) and a 5′-triphosphorylated RNA fragment (5′RF) with a 3′-side RNA fragment (3′RF) containing adenine or cytosine opposite the −1 position (Y = A or C). (*B*,*C*) Primer/template assay for simultaneously measuring the kinetics of nucleotide addition reactions by HsThg1 with two types of two-piece tRNA (Y = A or C). The reactions shown are time courses of activity with 10 µM HsThg1 and 0.1 mM GTP in excess over two-piece tRNA; aliquots from each time point were analyzed on urea-PAGE gels. RNA fragments were detected by SybrGold staining. Asterisk indicates upper bands which likely correspond to the G_{-2} addition to 5′RF/3′RF-A. (*D*) Time course experiments of the nucleotide addition reaction of HsThg1 with 3′RF-A (blue) or 3′RF-C (red). The bars in the graphs are SD of more than two independent experiments.

and showed that CaThg1 could add GTP to the 5′-end of 5′RF hybridized with 3′RF, forming a two-piece tRNA (Fig. 1A; Nakamura et al. 2018b). The two-piece tRNA (5′RF/3′RF) was useful for precise identification of single nucleotide elongation using polyacrylamide gel electrophoresis. In the current project we examined whether 5′RF/3′RF could be a substrate for HsThg1 as well as CaThg1. Cytoplasmic and mitochondrial tRNAs have A and C at the Y_{73} opposite to G_{-1} (Nakamura et al. 2018a). HsThg1 appears to be involved in the maturation of both tRNAs. Hence, 3′RFs with A_{73} and C_{73} at the Y position opposite to G_{-1} (3′RF-A, and 3′RF-C, Fig. 1A) were prepared, to reflect cytoplasmic and mitochondrial tRNAs (Fig. 1A–C). We investigated guanylylation activity, the second step of the G_{-1} addition reaction, using a triphosphorylated 5′RF in the presence of GTP, which can be incorporated without the adenylylation step, as previously reported (Jackman and Phizicky 2006; Smith and Jackman 2012; Nakamura et al. 2018b).

HsThg1 could transfer GTP to the 5′-end of 5′RF hybridized with 3′RF-A at an observed rate constant (k_{obs}) of 0.044 min^{-1} (Fig. 1B,D), which was slightly slower than the rate for full-length $tRNA^{His}$ (0.097 min^{-1}) previously determined (Hyde et al. 2010). As a result of hybridization with 3′RF-C, three GTP molecules (G_{-1}, G_{-2}, and G_{-3}) were incorporated at the 5′-end of 5′RF in the 3′–5′ direction (Fig. 1C), because a cytidine triplet was formed in the presence of 3′RF-C. The k_{obs} value of the nucleotide addition to 3′RF-C was 0.050 min^{-1}, comparable to that of 3′RF-A (Fig. 1D). We therefore confirmed that the two-piece tRNA could act as a substrate for HsThg1.

Addition of NTPs and GTP analogs by HsThg1

We investigated the incorporation of wild-type NTPs and GTP analogs (Fig. 2A) into 5′RF/3′RF-A or 5′RF/3′RF-C, and determined the k_{obs} value of each reaction (Table 1; Fig. 2B,C). In the presence of 3′RF-A template, HsThg1 added GTP and UTP to the 5′-end of the 5′RF but did not add ATP or CTP. The k_{obs} value for the addition of GTP was 2.5 times higher than that of UTP (Table 1; Fig. 2B). Only a single GTP was incorporated into the 5′-end opposite to A_{73}, and no further polymerization occurred, despite the presence of two cytidine residues (C_{74} and C_{75}) following A_{73} in the 3′RF-A. Although guanosine was able to pair with adenosine (Nakamura et al. 2018b), subsequent polymerization was prevented by the presence of the mismatched G_{-1}:A_{73} pair. It has been demonstrated that the rapid hydrolysis of the 5′-triphosphate from the mismatched G_{-1}:A_{73} pair on $tRNA^{His}$ is important to effectively terminate subsequent polymerization (Smith and Jackman 2014). The same mechanism could be used for the

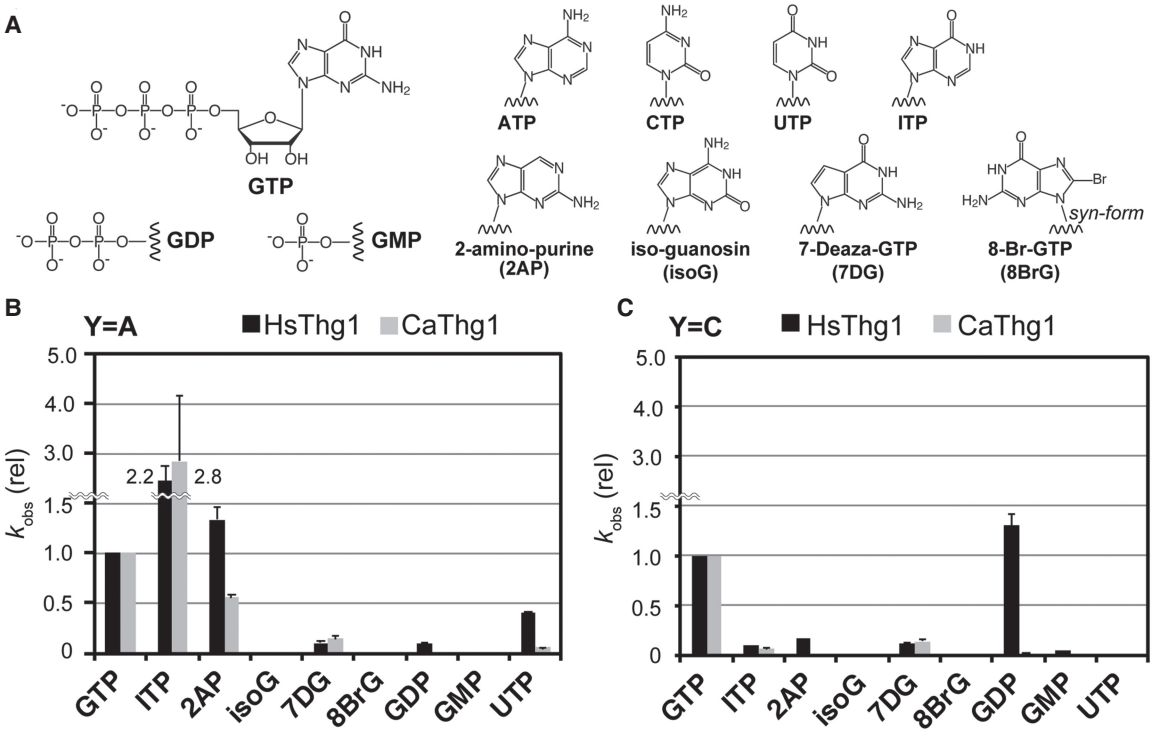

FIGURE 2. Addition activities of wild-type NTP and GTP analogs by HsThg1. (*A*) Natural NTPs and GTP analogs used in the nucleotide addition reaction. (*B*,*C*) The relative k_{obs} values of nucleotide addition reactions with various GTP analogs (0.1 mM) for the template Y = A (*B*), Y = C (*C*). Values are relative to the k_{obs} value of wild-type activity (GTP addition in Y = A). k_{obs} values of HsThg1 (this study) and CaThg1 (Nakamura et al. 2018b) are colored black and gray, respectively. The bars in the graphs are SD of more than two independent experiments.

TABLE 1. Comparison of the kinetics of nucleotide addition by HsThg1 and CaThg1 with NTP and various GTP analogs into two-piece tRNA

		k_{obs} (10^{-3} min^{-1})[a]								
Enzyme	Y	GTP	ITP	2AP	isoG	7DG	8BrG	GDP	GMP	UTP
HsThg1	A	44 ± 1.6 (1.0)[c]	96 ± 15 (2.2)	59 ± 5.1 (1.3)	N.D.[d]	4.3 ± 0.68 (0.098)	N.D.	4.1 ± 0.17 (0.093)	N.D.	18 ± 2.8 (0.41)
	C	50 ± 5.5 (1.1)	4.6 ± 0.01 (0.1)	8.0 ± 0.22 (0.18)	N.D.	5.8 ± 0.69 (0.13)	N.D.	65 ± 6.4 (1.5)	2.3 ± 0.03 (0.052)	N.D.
CaThg1[b]	A	65 ± 10 (1.0)[c]	180 ± 90 (2.8)	36 ± 2 (0.56)	N.D.	9.5 ± 2 (0.11)	N.D.	N.D.	N.D.	3.5 ± 0.2 (0.053)
	C	56 ± 10 (0.83)	3.6 ± 0.2 (0.056)	N.D.	N.D.	6.3 ± 1 (0.1)	N.D.	N.D.	N.D.	N.D.

Abbreviations of GTP analogs correspond to those shown in Figure 2A.
[a]Values reported are the average of at least three measurements.
[b]The k_{obs} values for GTP analogs using CaThg1 are taken from a previous report (Nakamura et al. 2018b).
[c]Values in parentheses are relative to the k_{obs} value of wild-type activity (GTP addition opposite A_{73}), which was set at 1.0.
[d]N.D. indicates values not determined.

5′RF/3′RF-A_{73}. This single GTP addition is consistently seen in the maturation of wild-type $tRNA^{His}$, providing a crucial element for HisRS in the cytoplasm of eukaryotes (Rudinger et al. 1994; Nameki et al. 1995; Rosen and Musier-Forsyth 2004).

To examine the exocyclic amino and keto groups of guanine, we investigated the incorporation of inosine triphosphate (ITP) and 2-aminopurine triphosphate (2AP) by HsThg1 (Table 1; Fig. 2B). Reactions involving ITP and 2AP were accelerated by 2.2 and 1.3 times over that of GTP, indicating that 6-keto and 2-amino groups are not essential for the HsThg1 reaction. However, isoguanine triphosphate (isoG), which contains 6-amino and 2-keto groups, was inactive, an observation which indicates that the isoguanine structure cannot be recognized by HsThg1. The k_{obs} value of 7-deazaguanosine triphosphate (7DG) was significantly decreased compared with that of GTP, indicating that the nitrogen atom at position 7 (N7) might be involved in binding the enzyme. 8-Br-GTP (8BrG), which adopts a *syn*-conformation (Kapuler and Reich 1971; Uno et al. 1971), did not produce any product. This observation, combined with the results obtained using other GTP analogs with *anti*-conformations, suggests that the *anti*-conformation is an absolute requirement for HsThg1-catalyzed reactions. GMP and GDP reactions were performed, and the triphosphate groups of GTP were investigated. GMP was not attached to the 5′-end of 5′RF-A, but GDP produced a small amount of product (Table 1; Fig. 2B). These results show that the triphosphate groups of GTP are needed for the HsThg1 reaction to occur when A_{73} is located opposite to G_{-1}.

We also examined the incorporation of GTP analogs in the presence of a 3′RF-C template incorporating cytidine (C_{73}, Fig. 1A) opposite G_{-1}. As discussed above, GTP had the same reaction rate as with a 3′RF-A template (Table 1; Fig. 2C) but the k_{obs} values of ITP and 2AP were decreased by nine- and sixfold. 7DG reacted at a very slow rate, and isoG was inactive, as observed using 3′RF-A. GDP and GMP could be incorporated into the 5′-end of 5′RF/3′RF-C. The reaction rate of GDP was slightly higher than that of GTP. We hypothesized that a G:C base pair was formed between the incoming GTP and the C_{73} on the 3′RF-C, resulting in stabilization of the binding of GTP to the enzyme. This G:C pairing would compensate for the lack of phosphate groups in the GTP.

It was recently reported that H152 and K187 in the active site of HsThg1 are involved in the GTP addition reaction with $tRNA^{His}$ containing A_{73}, but not with Watson–Crick G_{-1}:C_{73} or U_{-1}:A_{73} pairing, suggesting the possibility that HsThg1 uses two different mechanisms for GTP recognition depending on whether it is a WC or non-WC base-pairing (Matlock et al. 2019). We demonstrated that the triphosphate groups of GTP are essential for G_{-1}:A_{73} pairing, but not for G_{-1}:C_{73} pairing. These facts, taken together, indicate that HsThg1 can recognize GTP using either of two mechanisms: one involving non-WC pairing, and one involving WC base-pairing between GTP and the nucleobase (Y_{73}) of the template. In the case of G_{-1}:A_{73}, the G:A pair is unstable, but GTP binding to the active site of the enzyme is stabilized by interactions between the triphosphate group and conserved amino acids, as previously reported (Hyde et al. 2010; Nakamura et al. 2013). In the case of WC pairing, such as G_{-1}:C_{73}, the base-pairing acts primarily to stabilize the GTP binding to the active site of the enzyme.

Comparison between HsThg1- and CaThg1-catalyzing reactions

We compared the reaction profile of HsThg1 with that of *Candida albicans* Thg1 (CaThg1) (Table 1; Fig. 2B,C). The k_{obs} values of CaThg1 were determined in a previous study (Nakamura et al. 2018b). When 3′RF-A was used as a template, the reaction profiles of the GTP analogs ITP, 7DG,

isoG, and 8BrG were almost the same for the two enzymes, except for UTP. UTP was incorporated into the substrate about eight times faster by HsThg1 than by CaThg1. Although both enzymes can form non-WC G_{-1}:A_{73} and WC G_{-1}:C_{73} with similar activity (Table 1), both non-WC G_{-1}:A_{73}- and WC U_{-1}:A_{73} base pair formation occurred with HsThg1, whereas the non-WC G_{-1}:A_{73} base-pairing reaction was dominant with CaThg1. Furthermore, CaThg1 was inactive with GDP or GMP, even using 3′RF-C as a template, in contrast to HsThg1. These results suggest that CaThg1 strongly prefers GTP with its the triphosphate groups as an incoming nucleotide while HsThg1 is tolerant to UTP incorporation.

HsThg1 catalyzes the addition of G_{-1} to both human cytoplasmic (hc) and mitochondrial (hm) $tRNA^{His}$. Human cytoplasmic $tRNA^{His}$ contains A at the Y_{73} position, while mitochondrial $tRNA^{His}$ has C at this position (Nakamura et al. 2018a). CaThg1 is involved in the maturation of cytoplasmic $tRNA^{His}$ with an A_{73} but does not act on mitochondrial $tRNA^{His}$ because the G_{-1} of mitochondrial $tRNA^{His}$ in *C. albicans* is encoded in the mitochondrial genome the same as bacterial type $tRNA^{His}$. These results are consistent with those of our research. To produce both mature hc and hm $tRNA^{His}$, HsThg1 would have to exhibit both types of activity, forming mismatched G_{-1}:A_{73} and also forming WC base-pairing. CaThg1 would have to be adapted to form G_{-1}:A_{73} pairing for cytoplasmic $tRNA^{His}$ maturation. It has recently been reported that cytoplasmic $tRNA^{His}$ containing U_{-1} exists in BT-474 breast cancer cells and is enriched in the fraction of sex hormone-induced 5′-tRNA halves (Shigematsu and Kirino 2017). *Bombyx* Thg1 produces $tRNA^{His}$ containing U_{-1}, which is required for the expression of $tRNA^{His}$-derived piwi-interacting RNA (Honda et al. 2017). The preference of HsThg1 for WC base-pairing implies the existence of an unknown biological function, such as the biogenesis of noncoding RNAs.

5′-nucleotide addition activities of HsThg1 for application of 5′-end RNA labeling

The 3′-end of RNA can be modified with nucleotidyl or nonnucleotidyl molecules by enzymatic or chemical techniques (Bruce and Uhlenbeck 1978; England and Uhlenbeck 1978; Kojima et al. 2006). Postsynthetic modification of the 5′-end of RNA, however, is difficult. In order to apply HsThg1 to the 5′-end labeling of RNA, we incorporated GTP analogs, using a two-piece tRNA system (Fig. 3A). 3′RF-A and 3′RF-C enable single or multiple labeling (Fig. 3A). The GTP analogs 7-propargylamino- (proG), 7-biotin-propargylamino- (bioG), 2′-deoxy- (dGTP), 2′-*O*-methyl- (2meG), and 2′-azido (2azG)-GTPs were used (Fig. 3B). bioG labeling is used for the detection or capture of RNAs of interest, using specific interactions with a streptavidin or an avidin. proG can be used for postsynthetic modification of RNAs of interest. Labeling with 2meG or 2azG at the 5′-end of RNA can introduce nuclease resistance. The azido group of 2azG is also used for postsynthetic modification via click chemistry (Santner et al. 2014; Winz et al. 2018; Ganz et al. 2020).

5′RF/3′RF-A or 5′RF/3′RF-C complexes were incubated with GTP analogs in the presence of HsThg1 for 60 min, before the products were analyzed using gel electrophoresis (Fig. 3C,D). The percentages of labeled 5′RF are shown in Figure 3C,D. GTP provided 86% of the labeled RNA. bioG and proG could be added to the 5′-end of RNA with 15% and 32% efficiency, respectively. However, these GTP analogs were not incorporated by CaThg1 (Supplemental Fig. S1). For 2′-modifications, dGTP was incorporated with 64% efficiency, consistent with previous reports (Hyde et al. 2010), but the reaction products of 2meG were greatly reduced, to 8%. Bulky groups at the 2′-position of ribose might prevent the binding of GTP to the active site of HsThg1 by steric hindrance. HsThg1 could efficiently add 2azG to the 5′-end of the substrate RNA, since an azido group was available for click chemistry with an alkyne group. This observation suggests that various modifications can be introduced to the ribose moiety at the 5′-end of RNA in vitro and in vivo.

To perform multiple labeling of the 5′-end of RNA, we investigated the incorporation of GTP analogs in the presence of a 3′RF-C template (Fig. 3D). HsThg1 could add two bioG molecules to the 5′-end of substrate RNA corresponding to positions −1 and −2, with almost the same activity as GTP. The multiple incorporation efficiency of proG at the −1 and −2 position was 36%, which was almost identical to 3′RF-A. It is unclear why bioG, rather than proG, was preferentially incorporated at the 5′-end of the substrate RNA. In the presence of 3′RF-C template, multiple incorporation of the 2′-modified GTPs dGTP, 2meG, and 2azG could also be observed. Modifications of the 2′-position of GTP had little influence on the multiple incorporation, possibly because the G_{-1}:C_{73} base pair assisted the reaction. We also confirmed that full-length hc and hm $tRNA^{His}$ could be labeled with bioG by HsThg1 (Supplemental Fig. S2). These results from experiments with 7- and 2′-modified GTPs suggested that HsThg1 can be applied to the postsynthetic modification of the 5′-end of RNAs.

Structural diversity of the carboxy-terminal domains of the Thg1 family enzymes

HsThg1 transfers GTP to the 5′-end of both $hctRNA^{His}$ and $hmtRNA^{His}$. However, structural analysis of HsThg1 bound to $tRNA^{His}$ has not yet been performed. There is no structural information available for $hmtRNA^{His}$ recognition. We carried out cocrystallization of HsThg1 with $hmtRNA^{His}$, which contains the template base C opposite to the −1 position (Fig. 4A).

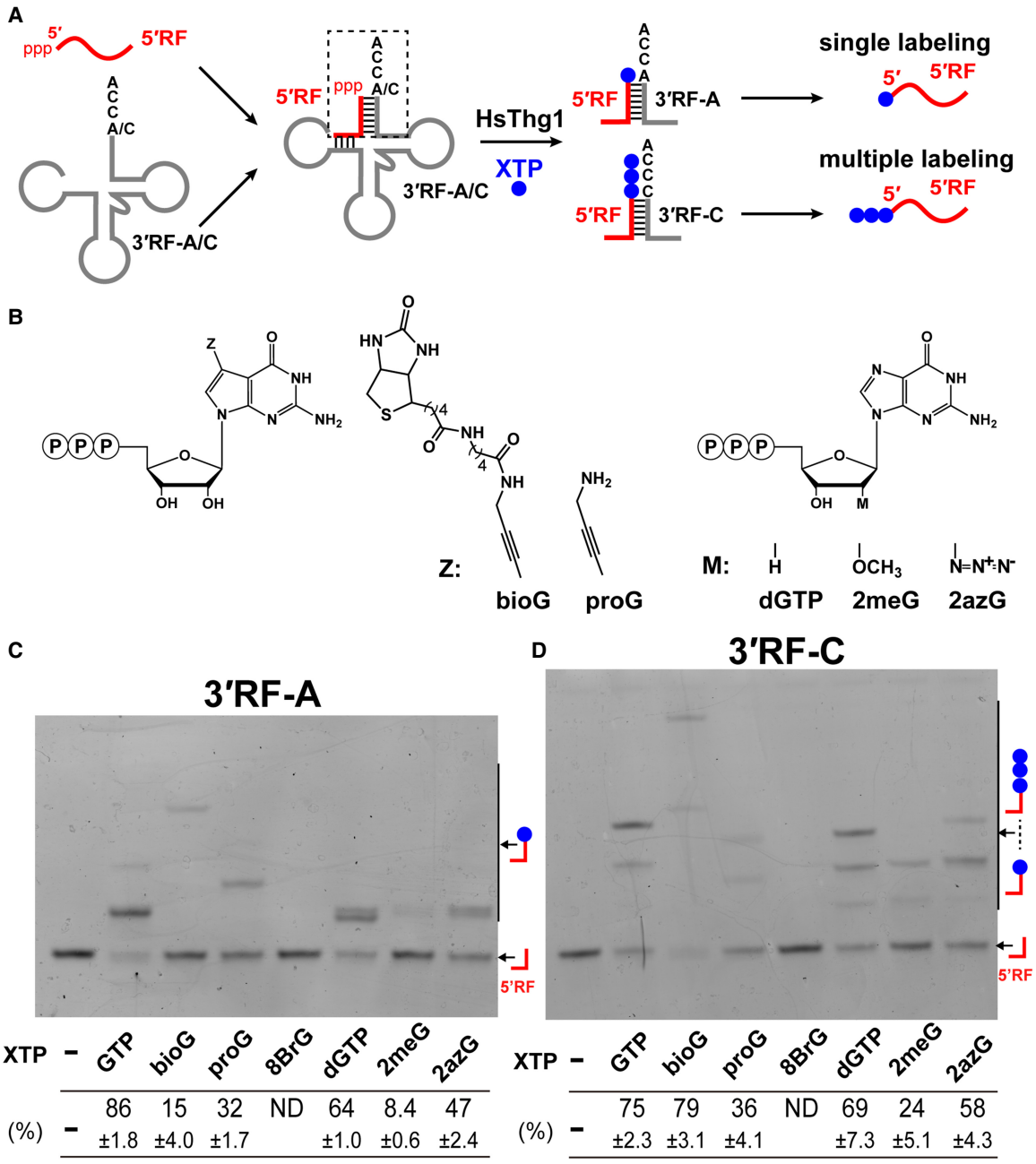

FIGURE 3. 5′-end RNA labeling with various GTP analogs by HsThg1. (*A*) Reaction scheme of single or multiple 5′-end RNA labeling by HsThg1 with 3′RF-A or 3′RF-C. HsThg1 adds single or multiple modified GTP analogs (XTP) to 5′-triphosphorylated 5′RF. (*B*) GTP analogs used in the 5′-end labeling reaction. Positions at which the GTP can be modified are indicated with Z (position 7) or M (2′OH). (*C*,*D*) Nucleotide addition by HsThg1 with various GTP analogs onto two-piece tRNA containing 3′RF-A (*C*) or 3′RF-C (*D*). The reaction mixture was incubated with HsThg1 and 1 mM modified GTP derivatives for 60 min and analyzed using urea-PAGE gels.

We determined the crystal structure of HsThg1 in the presence of hmtRNA^{His} at 4.0 Å resolution (Table 2). The crystal belongs to a trigonal space group ($P3_121$) and contains one tetramer of HsThg1 in an asymmetric unit (HsThg1-tetramer, Fig. 4B). The overall structure of the HsThg1-tetramer is very similar to the HsThg1-dimer structure previously determined (HsThg1-dimer, Fig. 4B; Hyde et al. 2010), except for a β-hairpin region at the carboxyl terminus. On the other hand, the carboxy-terminal domain of CaThg1 not bound to tRNA forms an α-helical structure rather than a β-hairpin (CaThg1-free, Fig. 4B; Nakamura et al. 2013). These comparisons reveal the structural diversity of the carboxy-terminal domains of these Thg1 enzymes.

There is no clear electron density map corresponding to the full-length hmtRNA^{His} in the asymmetric unit of

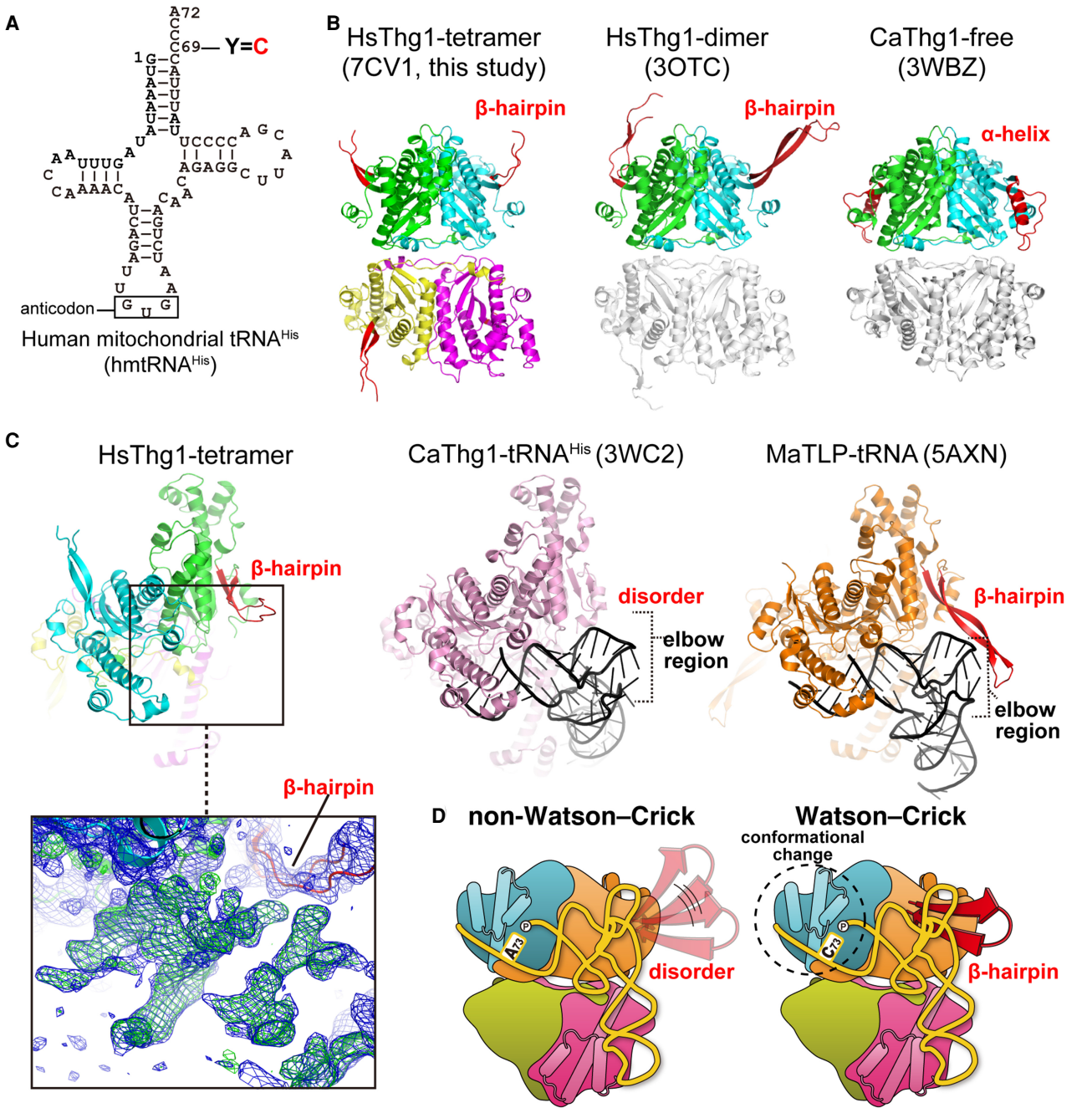

FIGURE 4. Structural comparison of Thg1 and TLP enzymes. (*A*) Human mitochondrial tRNA^{His} (hmtRNA^{His}) is drawn as a cloverleaf structure. hmtRNA^{His} contains a His-specific anticodon GUG and cytosine opposite the −1 position (Y = C). (*B*) Structural comparison of Thg1 enzymes: HsThg1 in the presence of hmtRNA^{His} (HsThg1-tetramer, this study), HsThg1-dimer (PDB ID: 3OTC) and CaThg1-free (PDB ID: 3WBZ), without tRNA^{His} binding. The flexibility of the β-hairpin structure at the carboxy-terminal of Thg1 is shown in red. (*C*) Structural comparison of Thg1 enzymes with tRNA binding: HsThg1 in the presence of hmtRNA^{His} (HsThg1-tetramer, this study), CaThg1-tRNA^{His} (PDB ID: 3WC2), and MaTLP-tRNA (PDB ID: 5AXN). The unknown electron density map (2Fo-Fc map [1.5 σ]; blue, and Fo-Fc map [2.5 σ]; green) close to the flexible β-hairpin is indicated as mesh. (*D*) Proposed incoming nucleotide recognition mechanism of HsThg1 organized by the interaction between the β-hairpin and the elbow region of the substrate tRNA.

HsThg1-tetramer; however, there is a residual electron density map close to the flexible β-hairpin region of only one monomer of HsThg1 (HsThg1-tetramer, Fig. 4C, inset). The structure of the cytoplasmic tRNA^{His}-bound CaThg1 (CaThg1-tRNA^{His}) has been reported (Nakamura et al. 2013). Superpositioning of the CaThg1-tRNA^{His} onto the HsThg1-tetramer shows that the interface region between the D-loop and T-loop (elbow region) of the tRNA^{His}

TABLE 2. Data collection and refinement statistics

	HsThg1 in the presence of hmtRNA^{His}
PDB ID	7CV1
Beam line	Photon Factory BL-1A
Wavelength (Å)	1.1000
Resolution range (Å)	50–4.0 (4.28–4.0)
Space group	$P\,3_1\,2\,1$
Unit cell (Å)	$a = b = 155.9$, $c = 201.5$
Total reflections	498,502 (93,005)
Unique reflections	24,468 (4363)
Multiplicity	20.4 (21.3)
Completeness (%)	100.0 (100.0)
Mean *I*/sigma(*I*)	5.9 (1.2)
Wilson B-factor (Å^2)	108.94
R-meas	1.036 (8.085)
$CC_{1/2}$	0.989 (0.547)
Reflections used in refinement	21,972
Reflections used for R_{free}	2431
R_{work}	0.2423
R_{free}	0.2554
Number of atoms	8211
Protein residues	986
RMS (bonds) (Å)	0.003
RMS (angles) (°)	0.53
Ramachandran favored (%)	98.45
Ramachandran allowed (%)	1.55
Ramachandran outliers (%)	0.00
Rotamer outliers (%)	0.00
Clashscore	7.15
Average B-factor (Å^2)	138.9
Number of TLS groups	1

Statistics for the highest-resolution shell are shown in parentheses.

superposes onto this map (Supplemental Fig. S3). These structural analyses suggest that the electron density map might correspond to the part of the elbow region of hmtRNA^{His} close to the flexible β-hairpin of HsThg1. It is unclear whether a part of hmtRNA^{His} was a degradation product of the full-length hmtRNA^{His} or other parts of hmtRNA^{His} were disordered in the crystal because of its flexibility.

The flexible β-hairpin of HsThg1 participates in the recognition of nucleotides to form Watson–Crick base pairs in 3′–5′ nucleotide addition

The carboxy-terminal domain of CaThg1 is completely disordered in the CaThg1-tRNA^{His} complex (CaThg1-tRNA^{His}, Fig. 4C). One more tRNA binding structure of the Thg1/TLP family enzymes has been reported—that of the *Methanosarcina acetivorans* TLP in complex with the 5′-end truncated tRNA (MaTLP-tRNA, Fig. 4C; Kimura et al. 2016). The carboxy-terminal domain of MaTLP forms a β-hairpin structure which binds to the elbow region of the substrate tRNA, in a manner similar to that of HsThg1 (MaTLP-tRNA, Fig. 4C). This interaction between the β-hairpin of MaTLP and tRNA is crucial for tRNA recognition without anticodon binding (Kimura et al. 2016). The structural diversity in the carboxy-terminal domain of enzymes of the Thg1/TLP family is strongly associated with the recognition of incoming nucleotides in the 3′–5′ nucleotide addition reaction. MaTLP is able to catalyze WC base pair-dependent nucleotide addition for the repair of the 5′-end of substrate tRNA, but not G:A mismatch formation for G_{-1} addition in cytoplasmic tRNA^{His} maturation (Abad et al. 2010, 2011). CaThg1 catalyzes the formation of G:A mismatches at the 5′-end of tRNA^{His} with 20-fold higher activity than WC U:A base-pairing by UTP addition (Jackman and Phizicky 2006; Nakamura et al. 2018b). Our biochemical data indicated that HsThg1 forms G:A mismatches, and also WC base-pairing, more efficiently than CaThg1 during 3′–5′ nucleotide addition. We propose the existence of two kinds of incoming nucleotide recognition mechanisms of HsThg1 (Fig. 4D). To form G:A mismatches, HsThg1 recognizes tRNA^{His} by anticodon binding, and does not need the β-hairpin to bind to tRNA^{His}, as does CaThg1 (Nakamura et al. 2013). To form WC base-pairing, the carboxy-terminal β-hairpin of HsThg1 binds to the elbow region of the substrate tRNA, affecting the position of the 5′-end of the substrate tRNA, and inducing a conformational change of active site residues such as H152 and K187, as discussed above.

Conclusion

In this study, we evaluated the efficiency of the incorporation of various nucleotide analogs into the −1 position by HsThg1, in a 3′–5′ direction. It has been proposed that there are two kinds of incoming nucleotide recognition mechanisms in HsThg1 depending on the base pair formation (Matlock et al. 2019). We also identified two kinds of incoming nucleotide recognition mechanisms; one is triphosphate binding-dependent G:A mismatch formation, and the other is strong WC base-pairing between the incoming nucleotide and the opposite template base, independent of triphosphate binding. We demonstrated that HsThg1 can be used for single or multiple labeling at the 5′-end of single-stranded RNA using two-piece tRNA with modified GTP analogs such as 7-biotinylated GTP. We also determined the crystal structure of HsThg1 in the presence of hmtRNA^{His}. From the structural comparison among the Thg1 family enzymes, the structural diversity of the carboxy-terminal domain of the Thg1 enzyme could be suggested and the conformational changes might be closely related to WC base-pairing in 3′–5′

nucleotide addition. These findings provide new insights into the previously unidentified biological functions of HsThg1, and are applicable to the 5′-terminal modification of RNAs.

MATERIALS AND METHODS

Preparation of HsThg1 and CaThg1

The amino-terminally His_6-tagged HsThg1 without a mitochondrial targeting sequence and CaThg1 were overexpressed in *E. coli* BL21 (DE3)-pRARE2 (Novagen), and purified as previously described (Nakamura et al. 2013, 2018a). Purified Thg1 enzymes were dialyzed against 25 mM HEPES-Na pH 7.5, 500 mM NaCl, 4 mM $MgCl_2$, 1 mM DTT, 50% (v/v) glycerol. Dialyzed samples were concentrated to a final concentration of 170–190 µM, and stored at −30°C

Preparation of 3′RFs and full-length tRNAs

5′-truncated *S. cerevisiae* $tRNA^{Phe}_{GUG}$ fragments (3′RFs), and hm and hc $tRNA^{His}$ variants were transcribed using T7 RNA polymerase as described previously (Nakamura et al. 2018a,b). Double-stranded DNAs encoding the T7 promoter and target RNA sequences were amplified by PCR with three overlapping primers and cloned into the *BamHI*/*HindIII* site of pUC19. The inserted sequences were verified by DNA sequencing. Double-stranded DNA transcription templates were obtained by PCR and were purified using a GenElute PCR Clean-Up kit (Sigma). The in vitro transcription was performed using a DuraScribe T7 Transcription kit (Epicentre) at 37°C for 6 h. The reaction mixture was subsequently treated with DNase I at 37°C for 30 min to degrade the template DNA and purified using 10% denaturing urea-polyacrylamide gel electrophoresis (Urea-PAGE). RNAs were extracted from gel slices and refolded simultaneously in H_2O at 4°C for 18 h. The extracted RNA samples were precipitated with ethanol, dissolved in TE buffer pH8.0, and stored at −80°C.

Preparation of 5′-triphosphorylated 5′RF

The 5′-triphosphorylated 5′RF (13 nts) was synthesized by in vitro transcription as described previously (Nakamura et al. 2018b). The following DNA oligonucleotides were used for preparation of a transcription template: T7 promoter D, 5′-GGAATTGGATC CTAATACGACTCACTATAG; template strand, 5′-GAGCTAAAT CCGCTATAGTGAGTCGTATTAGGATCCAATTCC. The transcription template was prepared by heating the two DNA strands together to 95°C for 5 min and allowing to gradually cool to 25°C. The in vitro transcription was performed by using a DuraScribe T7 Transcription kit at 37°C for 6 h. The transcribed RNA was purified by 20% (w/v) Urea-PAGE and extracted in H_2O at 4°C for 18 h. The extracted RNA was loaded onto a reverse-phase column (YMC) preequilibrated with H_2O. The column was washed with H_2O, and the RNA was eluted with 50% acetonitrile. Elution fractions were dried up and disolved in H_2O, and stored at −80°C.

Nucleotide addition assay using two-piece tRNAs

Two-piece tRNAs for nucleotide addition assays were constructed by annealing of a 5′RF and a 3′RF. Annealing conditions for all the two-piece tRNAs were as follows: a mixture of 1 µM of the primer RNA and 2.5 µM of template RNA in 25 mM HEPES-Na pH 7.5, 125 mM NaCl, 10 mM $MgCl_2$, 2 mM spermidin HCl was incubated at 65°C for 2 min, then gradually cooled to 25°C. Reactions contained the annealed two-piece tRNA in 25 mM HEPES-Na pH 7.5, 125 mM NaCl, 10 mM $MgCl_2$, 3 mM DTT, 2 mM spermidin HCl, and 0.1 mM NTP or GTP analogs for nucleotide addition reactions, and were preincubated at 25°C for 5 min, and intiated by addition of a saturating concentration of enzyme (10 µM). At various time points, aliquots (1 µL) were mixed with an equal volume of loading buffer (10 M urea, 50 mM EDTA, and 0.1% bromophenol blue), and analyzed by 20% Urea-PAGE. The gels were stained with SYBR Gold Nucleic Acid Gel Stain (Thermo Fisher Scientific) and visualized and quantified using Typhoon and Image Quant software (GE Healthsciences). Single-turnover rate constants (k_{obs}) and maximal product formation (P_{max}) were determined as previously reported (Smith and Jackman 2012; Nakamura et al. 2018b). Time courses of product formation were plotted and fit to a single-exponential rate equation: $Pt = P_{max}[1 - \exp(-k_{obs}t)]$ (Equation 1), where Pt is the fraction of product formed at each time, and P_{max} is the maximum amount of product conversion observed during each time course. To evaluate incorporation acitivity of Thg1 enzymes for modified GTP derivatives such as 7-biothinylated GTP, reaction mixture was incubated with Thg1 and 1 mM modified GTP derivatives for 60 min, and analyzed by Urea-PAGE gel, as described above. All reported parameters were determined from at least two independent experiments.

Crystallization and data collection of HsThg1 with $hmtRNA^{His}$

HsThg1 and $hmtRNA^{His}$ were mixed in a molecular ratio of 1:1 in buffer C (80 µM each). Crystals of HsThg1 with $hmtRNA^{His}$ were obtained by sitting drop vapor diffusion against 0.1 M Tris-HCl pH 7.0, 10% (w/v) PEG6000, 5% (w/v) Tacsimate pH7.0 at 20°C. The diffraction data set of HsThg1 with $hmtRNA^{His}$ was collected on beamline BL1A (Photon Factory) with a wavelength of 1.1000 Å at −173°C after crystals were soaked into reservoir solution buffer containing 30% (v/v) glycerol. Diffraction data set of HsThg1 with $hmtRNA^{His}$ was integrated with *DIALS* (Waterman et al. 2016) and scaled with *AIMLESS* (Evans and Murshudov 2013). The data-collection statistics are shown in Table 2.

Structure determination and refinement

The structure of HsThg1 with $hmtRNA^{His}$ was solved by molecular replacement using *phaser* in the *CCP4* suite (McCoy et al. 2007), with the dimer structure of HsThg1 (PDB ID: 3OTE) (Hyde et al. 2010) as a search model. The model of HsThg1 was modified manually using *Coot* (Emsley et al. 2010). Structure refinement was performed using *phenix.refine* (Afonine et al. 2012) and *autoBUSTER* (Blanc et al. 2004) with noncrystallographic symmetry restraints. Finally, R_{work}- and R_{free}-factors were converged to 24.2% and 25.5%, respectively (Table 2). Ramachandran plots of all determined structures were calculated using *MolProbity*

(Chen et al. 2010), and showed that 98.5% of the protein residues were in the favored regions, with no residues in the outlier region. The refinement statistics are shown in Table 2. All figures were prepared with *PyMOL* (The PyMOL Molecular Graphics System, Version 1.5.0.4).

DATA DEPOSITION

The structures of HsThg1 in the presence of hmtRNA^{His} were deposited to the Protein Data Bank with PDB ID 7CV1.

SUPPLEMENTAL MATERIAL

Supplemental material is available for this article.

ACKNOWLEDGMENTS

We thank Drs. Eiko Ohtsuka, Yasuhiro Mie, Yu Hirano, and Mashiki Ikegami (AIST) for helpful insights, Keitaro Yamashita (MRC Laboratory of Molecular Biology) for advice on data processing and structure analysis. We also acknowledge the beamline staff at Photon Factory for their kind support in the X-ray diffraction experiments (2018G084). This work was supported by the Japan Society for the Promotion of Science (JSPS) KAKENHI grant number 16K18511 (to A.N.) and 19K06519 (to A.N.).

Received November 4, 2020; accepted March 21, 2021.

REFERENCES

Abad MG, Rao BS, Jackman JE. 2010. Template-dependent 3′-5′ nucleotide addition is a shared feature of tRNA^{His} guanylyltransferase enzymes from multiple domains of life. *Proc Natl Acad Sci* **107:** 674–679. doi:10.1073/pnas.0910961107

Abad MG, Long Y, Willcox A, Gott JM, Gray MW, Jackman JE. 2011. A role for tRNA^{His} guanylyltransferase (Thg1)-like proteins from *Dictyostelium discoideum* in mitochondrial 5′-tRNA editing. *RNA* **17:** 613–623. doi:10.1261/rna.2517111

Afonine P V, Grosse-Kunstleve RW, Echols N, Headd JJ, Moriarty NW, Mustyakimov M, Terwilliger TC, Urzhumtsev A, Zwart PH, Adams PD. 2012. Towards automated crystallographic structure refinement with phenix.refine. *Acta Crystallogr D Biol Crystallogr* **68:** 352–367. doi:10.1107/S0907444912001308

Blanc E, Roversi P, Vonrhein C, Flensburg C, Lea SM, Bricogne G. 2004. Refinement of severely incomplete structures with maximum likelihood in BUSTER-TNT. *Acta Crystallogr D Biol Crystallogr* **60:** 2210–2221. doi:10.1107/S0907444904016427

Bruce AG, Uhlenbeck OC. 1978. Reactions at the termini of tRNA with T4 RNA ligase. *Nucleic Acids Res* **5:** 3665–3678. doi:10.1093/nar/5.10.3665

Chen VB, Arendall WB, Headd JJ, Keedy DA, Immormino RM, Kapral GJ, Murray LW, Richardson JS, Richardson DC. 2010. MolProbity: all-atom structure validation for macromolecular crystallography. *Acta Crystallogr D Biol Crystallogr* **66:** 12–21. doi:10.1107/S0907444909042073

Chen AW, Jayasinghe MI, Chung CZ, Rao BS, Kenana R, Heinemann IU, Jackman JE. 2019. The role of 3′ to 5′ reverse RNA polymerization in tRNA fidelity and repair. *Genes (Basel)* **10:** 250. doi:10.3390/genes10030250

Cooley L, Appel B, Söll D. 1982. Post-transcriptional nucleotide addition is responsible for the formation of the 5′ terminus of histidine tRNA. *Proc Natl Acad Sci* **79:** 6475–6479. doi:10.1073/pnas.79.21.6475

Dodbele S, Moreland B, Gardner SM, Bundschuh R, Jackman JE. 2019. 5′-end sequencing in *Saccharomyces cerevisiae* offers new insights into 5′-ends of tRNA^{His} and snoRNAs. *FEBS Lett* **593:** 971–981. doi:10.1002/1873-3468.13364

Emsley P, Lohkamp B, Scott WG, Cowtan K. 2010. Features and development of Coot. *Acta Crystallogr D Biol Crystallogr* **66:** 486–501. doi:10.1107/S0907444910007493

England TE, Uhlenbeck OC. 1978. 3′-Terminal labelling of RNA with T4 RNA ligase. *Nature* **275:** 560–561. doi:10.1038/275560a0

Evans PR, Murshudov GN. 2013. How good are my data and what is the resolution? *Acta Crystallogr Sect D Biol Crystallogr* **69:** 1204–1214. doi:10.1107/S0907444913000061

Ganz D, Harijan D, Wagenknecht H-A. 2020. Labelling of DNA and RNA in the cellular environment by means of bioorthogonal cycloaddition chemistry. *RSC Chem Biol* **1:** 86–97. doi:10.1039/D0CB00047G

Gu W, Jackman JE, Lohan AJ, Gray MW, Phizicky EM. 2003. tRNA^{His} maturation: an essential yeast protein catalyzes addition of a guanine nucleotide to the 5′ end of tRNA^{His}. *Genes Dev* **17:** 2889–2901. doi:10.1101/gad.1148603

Heinemann IU, Randau L, Tomko RJ Jr, Söll D. 2010. 3′-5′ tRNA^{His} guanylyltransferase in bacteria. *FEBS Lett* **584:** 3567–3572. doi:10.1016/j.febslet.2010.07.023

Heinemann IU, Nakamura A, O'Donoghue P, Eiler D, Söll D. 2012. tRNA^{His}-guanylyltransferase establishes tRNA^{His} identity. *Nucleic Acids Res* **40:** 333–344. doi:10.1093/nar/gkr696

Himeno H, Hasegawa T, Ueda T, Watanabe K, Miura K, Shimizu M. 1989. Role of the extra G-C pair at the end of the acceptor stem of tRNA^{His} in aminoacylation. *Nucleic Acids Res* **17:** 7855–7863. doi:10.1093/nar/17.19.7855

Honda S, Kawamura T, Loher P, Morichika K, Rigoutsos I, Kirino Y. 2017. The biogenesis pathway of tRNA-derived piRNAs in Bombyx germ cells. *Nucleic Acids Res* **45:** 9108–9120. doi:10.1093/nar/gkx537

Hyde SJ, Eckenroth BE, Smith BA, Eberley WA, Heintz NH, Jackman JE, Doublié S. 2010. tRNA^{His} guanylyltransferase (THG1), a unique 3′-5′ nucleotidyl transferase, shares unexpected structural homology with canonical 5′–3′ DNA polymerases. *Proc Natl Acad Sci* **107:** 20305–20310. doi:10.1073/pnas.1010436107

Jackman JE, Phizicky EM. 2006. tRNA^{His} guanylyltransferase catalyzes a 3′–5′ polymerization reaction that is distinct from G_{-1} addition. *Proc Natl Acad Sci* **103:** 8640–8645. doi:10.1073/pnas.0603068103

Jackman JE, Gott JM, Gray MW. 2012. Doing it in reverse: 3′-to-5′ polymerization by the Thg1 superfamily. *RNA* **18:** 886–899. doi:10.1261/rna.032300.112

Jahn D, Pande S. 1991. Histidine tRNA guanylyltransferase from *Saccharomyces cerevisiae*. II. Catalytic mechanism. *J Biol Chem* **266:** 22832–22836. doi:10.1016/S0021-9258(18)54429-X

Kapuler AM, Reich E. 1971. Some stereochemical requirements of *Escherichia coli* ribonucleic acid polymerase. Interaction with conformationally restricted ribonucleoside 5′-triphosphates: 8-bromoguanosine, 8-ketoguanosine, and 6-methylcytidine triphosphates. *Biochemistry* **10:** 4050–4061. doi:10.1021/bi00798a007

Kimura S, Suzuki T, Chen M, Kato K, Yu J, Nakamura A, Tanaka I, Yao M. 2016. Template-dependent nucleotide addition in the reverse (3′–5′) direction by Thg1-like protein. *Sci Adv* **2:** e1501397. doi:10.1126/sciadv.1501397

Kojima N, Sugino M, Mikami A, Nonaka K, Fujinawa Y, Muto I, Matsubara K, Ohtsuka E, Komatsu Y. 2006. Enhanced reactivity of amino-modified oligonucleotides by insertion of aromatic residue. *Bioorganic Med Chem Lett* **16:** 5118–5121. doi:10.1016/j.bmcl.2006.07.027

Lee YH, Chang CP, Cheng YJ, Kuo YY, Lin YS, Wang CC. 2017. Evolutionary gain of highly divergent tRNA specificities by two isoforms of human histidyl-tRNA synthetase. *Cell Mol Life Sci* **74:** 2663–2677. doi:10.1007/s00018-017-2491-3

Lee YH, Lo YT, Chang CP, Yeh CS, Chang TH, Chen YW, Tseng YK, Wang CC. 2019. Naturally occurring dual recognition of $tRNA^{His}$ substrates with and without a universal identity element. *RNA Biol* **16:** 1275–1285. doi:10.1080/15476286.2019.1626663

Long Y, Abad MG, Olson ED, Carrillo EY, Jackman JE. 2016. Identification of distinct biological functions for four 3′–5′ RNA polymerases. *Nucleic Acids Res* **44:** 8395–8406. doi:10.1093/nar/gkw681

Matlock AO, Smith BA, Jackman JE. 2019. Chemical footprinting and kinetic assays reveal dual functions for highly conserved eukaryotic $tRNA^{His}$ guanylyltransferase residues. *J Biol Chem* **294:** 8885–8893. doi:10.1074/jbc.RA119.007939

McCoy AJ, Grosse-Kunstleve RW, Adams PD, Winn MD, Storoni LC, Read RJ. 2007. Phaser crystallographic software. *J Appl Crystallogr* **40:** 658–674. doi:10.1107/S0021889807021206

Nakamura A, Nemoto T, Heinemann IU, Yamashita K, Sonoda T, Komoda K, Tanaka I, Söll D, Yao M. 2013. Structural basis of reverse nucleotide polymerization. *Proc Natl Acad Sci* **110:** 20970–20975. doi:10.1073/pnas.1321312111

Nakamura A, Wang D, Komatsu Y. 2018a. Biochemical analysis of human $tRNA^{His}$ guanylyltransferase in mitochondrial $tRNA^{His}$ maturation. *Biochem Biophys Res Commun* **503:** 2015–2021. doi:10.1016/j.bbrc.2018.07.150

Nakamura A, Wang D, Komatsu Y. 2018b. Molecular mechanism of substrate recognition and specificity of $tRNA^{His}$ guanylyltransferase during nucleotide addition in the 3′–5′ direction. *RNA* **24:** 1583–1593. doi:10.1261/rna.067330.118

Nameki N, Asahara H, Shimizu M, Okada N, Himeno H. 1995. Identity elements of *Saccharomyces cerevisiae* $tRNA^{His}$. *Nucleic Acids Res* **23:** 389–394. doi:10.1093/nar/23.3.389

Rao BS, Jackman JE. 2015. Life without post-transcriptional addition of G_{-1}: two alternatives for $tRNA^{His}$ identity in Eukarya. *RNA* **21:** 243–253. doi:10.1261/rna.048389.114

Rao BS, Maris EL, Jackman JE. 2011. tRNA 5′-end repair activities of $tRNA^{His}$ guanylyltransferase (Thg1)-like proteins from Bacteria and Archaea. *Nucleic Acids Res* **39:** 1833–1842. doi:10.1093/nar/gkq976

Rosen AE, Musier-Forsyth K. 2004. Recognition of G-1:C73 atomic groups by *Escherichia coli* histidyl-tRNA synthetase. *J Am Chem Soc* **126:** 64–65. doi:10.1021/ja0381609

Rudinger J, Florentz C, Giegé R. 1994. Histidylation by yeast HisRS of tRNA or tRNA-like structure relies on residues −1 and 73 but is dependent on the RNA context. *Nucleic Acids Res* **22:** 5031–5037. doi:10.1093/nar/22.23.5031

Santner T, Hartl M, Bister K, Micura R. 2014. Efficient access to 3′-terminal azide-modified RNA for inverse click-labeling patterns. *Bioconjug Chem* **25:** 188–195. doi:10.1021/bc400513z

Shigematsu M, Kirino Y. 2017. 5′-terminal nucleotide variations in human cytoplasmic $tRNA^{HisGUG}$ and its 5′-halves. *RNA* **23:** 161–168. doi:10.1261/rna.058024.116

Smith BA, Jackman JE. 2012. Kinetic analysis of 3′–5′ nucleotide addition catalyzed by eukaryotic $tRNA^{His}$ guanylyltransferase. *Biochemistry* **51:** 453–465. doi:10.1021/bi201397f

Smith BA, Jackman JE. 2014. *Saccharomyces cerevisiae* Thg1 uses 5′-pyrophosphate removal to control addition of nucleotides to $tRNA^{His}$. *Biochemistry* **53:** 1380–1391. doi:10.1021/bi4014648

Suzuki T, Suzuki T. 2014. A complete landscape of post-transcriptional modifications in mammalian mitochondrial tRNAs. *Nucleic Acids Res* **42:** 7346–7357. doi:10.1093/nar/gku390

Uno H, Oyabu S, Otsuka E, Ikehara M. 1971. The effect of guanosine 5′-triphosphate analogues on protein synthesis. *Biochim Biophys Acta* **228:** 282–288. doi:10.1016/0005-2787(71)90568-5

Waterman DG, Winter G, Gildea RJ, Parkhurst JM, Brewster AS, Sauter NK, Evans G. 2016. Diffraction-geometry refinement in the DIALS framework. *Acta Crystallogr Sect D Struct Biol* **72:** 558–575. doi:10.1107/S2059798316002187

Winz ML, Linder EC, Becker J, Jäschke A. 2018. Site-specific one-pot triple click labeling for DNA and RNA. *Chem Commun* **54:** 11781–11784. doi:10.1039/C8CC04520H